

# Adsorption and calorimetric studies of hydrothermally modified carbosils

Barbara Charmas

Received: 29 July 2013 / Accepted: 11 October 2013 / Published online: 30 October 2013  
© The Author(s) 2013. This article is published with open access at Springerlink.com

**Abstract** The article presents the studies of effects of hydrothermal treatment (HTT) (in saturated water vapours or under the liquid water layer) using various sources of thermal energy (classical autoclave or high pressure microwave reactor) on structural and surface properties of initial and modified silica gels and carbon–silica adsorbents. The porous structure of the initial and modified materials was characterised by the low-temperature nitrogen adsorption/desorption method as well as by determining pore volume distribution curves from the calorimetric data (DSC) using the thermal effects of liquid (water) phase transitions previously brought inside the pores of the studied materials. Large compatibility of the characteristics obtained using the above methods was found. The microscopic investigations (SEM, TEM) were also conducted to evaluate the morphology and topography of the samples. It was proved that during HTT, the carbon deposit on the silica surface screens it against the access of water molecules, in this way affecting decrease in intensity of dissolution and condensation of polysilicic acids. At the same time, owing to oxidizing properties of water molecules under hydrothermal conditions, development of porous structure in the carbon deposit is observed. Extent of these changes depends on both the applied system (water vapour/liquid water) and kind of the used energy (classical/microwave).

**Keywords** Carbon–mineral adsorbents · Hydrothermal modification · Thermogravimetry · Differential scanning calorimetry · Porous structure

## Introduction

Carbon–silica adsorbents (carbosils) are composite materials of numerous applications [1–4]. Their applicability results mainly from their original surface properties combining the characteristics of both nonpolar carbon and polar mineral parts (e.g. the nature of adsorption sites such as the Brønsted and Lewis acid sites, pore structure and surface heterogeneity) [3, 5–7] desired for different adsorption processes. Such adsorbents can be used in water and waste water purification processes, because they can adsorb organic and inorganic substances simultaneously [1–4, 8–13].

Carbosils can be used also as catalyst carriers, often working under the conditions resembling the hydrothermal ones. Therefore they should possess suitable physical and chemical properties (high thermal resistance, mechanical strength, proper sorption capacity and phase composition, well defined and stable surface character etc.). It is possible to obtain these advantageous properties using hydrothermal treatment (HTT) [11–15]. This way of carbosils surface modification is one of the most effective methods enabling formation of new properties of such materials. During HTT of silica materials, silica mass transfer process occurs due to its dissolution and re-condensation [16]. The smallest silica particles characterised by the maximal surface energy are dissolved as the first, due to the largest chemical potential. As a result, silica is transferred and deposits on larger particles, whose surface energy and chemical potential are smaller. Consequently, intensive changes in

B. Charmas (✉)  
Department of Chromatographic Methods, Faculty of Chemistry,  
Maria Curie-Skłodowska University, Maria Curie-Skłodowska  
Sq. 3, 20-031 Lublin, Poland  
e-mail: barbara@charmas.pl

the structure of silica skeleton and then in porous structure are found. In the case of composite materials, the presence of carbon deposit restrains significantly the effect of hydrothermal modification on the surface and structural properties of the initial silica. At the same time, HTT causes changes in the porous structure of carbon deposit itself and also changes the number and character of functional groups of the materials under modification [11–15].

Hydrothermal modification of adsorbents and catalysts consists in the reaction of water (in the gaseous or liquid phase) molecules with the modified material at the temperature over 100 °C under the increased pressure. Under these conditions water changes its properties due to decay of the original tetrahedral structure. As a result, its ability of solid dissolution increases. Silica gels are particularly susceptible to the action of water vapour under such conditions [16]. Effectiveness of the HTT process depends on the structure of the initial adsorbent, temperature, time and process conditions (gaseous or liquid phase, pH) [11–15].

Changes in the porous structure and surface character taking place under the HTT influence affect the character of water molecules with pores surface interactions [17–20]. Making use of differential scanning calorimetry (DSC) to study the behaviour of water molecules inside pores of the materials provides significant information about their porous structure [21–28]. The assumptions of the method are based on the analysis of phase transitions of liquid media inside the pores. This method was introduced for the first time by Brun et al. [29] laying down the thermodynamic bases for calorimetric determination of porous materials structure from the thermal effects connected with freezing/melting of liquids in pores. These assumptions were based on the observations of changes of freezing/melting points of different liquids contained in pores. It was shown that these changes are closely connected with the size of pores in the studied materials [30, 31]. The authors [29] exploited the fact that in the mesoporous material pores, there can occur water of two kinds i.e. water freezing in the pores (forming ice crystals, unbound or weakly bound with the pores surface) and non-freezing water (which cannot undergo phase transformation during freezing or melting, strongly bound with pores surface). This is the reason for the differences in the observed temperature ( $T_{\max}$ ,  $T_{\text{onset}}$ ) and thermal effects ( $\Delta H$ ) during liquid–water freezing and ice crystals melting inside the porous structure.

In this study, the adsorption ( $N_2$ ), calorimetric (DSC) and thermal (TG) investigations were performed to evaluate the porous structure of carbosils modified hydrothermally under different conditions (classical autoclave or microwave reactor) and media (liquid water and water vapour). The knowledge of the structural characteristics makes it possible to use these materials in different practical fields. The aim was to establish the relationships

between the conditions of the modification process, structural parameters and properties of the hydrothermally modified adsorbents.

## Experimental

### Preparation of adsorbents

Carbosils were prepared by  $\text{CH}_2\text{Cl}_2$  pyrolysis on the silica gel surface (Si-60, Merck) using the rotary reactor. The pyrolysis process was conducted at 550 °C in the nitrogen atmosphere for the period from 0.5 to 6 h (the samples were denoted CS- $x$  respectively, where  $x = 1$ –6). Extension of pyrolysis time made it possible to prepare materials increasing in carbon deposit content ( $C_C$  in the range of 1.8–19 %).

### Modification of adsorbents

#### *Modification in the classical autoclave*

Hydrothermal modification of carbosils was conducted in the steel autoclave in the saturated water vapour atmosphere (the samples CS- $x_{\text{a-vap}}$ , where “a” means modification in the autoclave and “vap” in the water vapour atmosphere) or under the layer of liquid water (the samples CS- $x_{\text{a-liq}}$ , where “liq” means modification under the layer of liquid water) at 200 °C, 6 h. Under the same conditions, the initial silica gel was modified and denoted Si-60 $_{\text{a-vap}}$  and Si-60 $_{\text{a-liq}}$ , respectively.

#### *Modification in the microwave reactor*

Hydrothermal modification of carbosils was made in the high-pressure microwave reactor (Plazmatronika, Poland) in the saturated water vapour atmosphere (the samples CS- $x_{\text{m-vap}}$ , where “m” means modification in the microwave reactor and “vap” in the water vapour atmosphere) or under the layer of liquid water (the samples CS- $x_{\text{m-liq}}$ , where “liq” means modification in the presence of liquid water) at 200 °C for 1 h. Under the same conditions, the initial silica gel was modified and denoted Si-60 $_{\text{m-vap}}$  and Si-60 $_{\text{m-liq}}$ , respectively.

#### *Thermal modification of carbosils*

In order to examine the screening effect of carbon deposit present on the carbosils surface against the action of overheated water vapour during the HTT, the samples modified in the autoclave in the saturated water vapour (CS- $x_{\text{a-vap}}$ ) atmosphere were additionally subjected to thermal treatment at 500 °C. In this way the carbon deposit

was removed, and the obtained silica gels were denoted CS- $x_{a-vap-T}$ . For comparison, the initial silica gel was also treated in the same way and denoted Si-60 $_{a-vap-T}$ . The detailed parameters of preparation and modification are described in the article [21].

## Research methods

To characterise structural and thermal properties of the studied carbosils, there were applied the following methods: low-temperature nitrogen adsorption/desorption method; derivatographic analyses TG, DTG and DTA; DSC in the temperature range from  $-40$  to  $30$  °C and microscopic analyses (SEM, TEM). For calculation of structural parameters, there were used low-temperature ( $-196$  °C) nitrogen adsorption/desorption isotherms data (Micromeritics, ASAP 2405N, Norcross, USA). The specific surface area was calculated according to the standard BET method [32]. The total pore volume was estimated under the relative pressure  $p/p_0 = 0.98-0.99$ . To compute the pore size distributions desorption data were used. The proposed computation is based on the use of regularization procedure under non-negativity conditions for the pore size distribution function ( $f(R_p) > 0$  at any pore radius  $R_p$ ) at the fixed regularization parameter  $\alpha = 0.01$ . The pore size distributions for silicas have been calculated assuming the cylindrical shape of pores. To show a complex shape of carbosil pores, the SC-model with voids between the nanoparticles (SCV-model) using the SCR procedure [33] modified by the Nguyen-Do [34] method was applied. The SCV/SCR method allows us to estimate the contribution of different types of pores into the total porosity [35]. The differential PSD functions with respect to the pore volume (PSD $_v$ ,  $dV/dR = f(R_p)$ ) were applied to estimate the contribution of different types of pores: nanopores ( $V_{nano}$ ,  $S_{nano}$  at  $R_p < 1$  nm), mesopores ( $V_{meso}$ ,  $S_{meso}$  at  $1$  nm  $< R_p < 25$  nm) and macropores ( $V_{macro}$ ,  $S_{macro}$  at  $R_p > 25$  nm) [25, 30, 34, 36–38].

The derivatographic measurements were made using Derivatograph-C (Paulik, Paulik and Erdey, Budapest, Hungary). The investigations were carried out with the linear temperature accretion ( $10$  °C  $\text{min}^{-1}$ ) in the air atmosphere and the temperature range of  $20-1,000$  °C. From the obtained results, the carbon deposit ( $C_c$ ) content was determined in the carbosil samples [21].

Calorimetric studies were carried out using differential scanning calorimetry (DSC PYRIS Diamond, Perkin Elmer, USA). Before the studies the samples were saturated with water vapour in the desiccator at room temperature for 72 h. The extent of saturation with water was determined from the thermogravimetric (TG) measurements conducted in the range of  $20-300$  °C. The weighed

samples were closed in the aluminium cells. The DSC studies of water freezing for all samples were carried out in the temperature range from  $+30$  to  $-40$  °C at the linear rate of temperature change  $10$  °C  $\text{min}^{-1}$ . The empty crucible was the standard sample. Helium was used as the curtain gas. During the studies there were registered the ice melting curves which were used for determination of characteristic temperatures  $T_{max}$ ,  $T_{onset}$  as well as enthalpy  $\Delta H$  of the ongoing processes. It is assumed that  $T_{max}$  corresponds to the phase transformations of ice melting in the pores of the sizes  $R_{av}$ . However, the phase transitions occurring in the pores of the size  $R_{min}$  correspond to the temperature of peak start,  $T_{onset}$ . It should be noted that the size and width of the peak on the DSC curve also depend on the liquid mass in the analysed sample and the rate of temperature changes [39].

The DSC data obtained due to melting of the ice confined in the pores were used for determination of sizes of water clusters, nano- and microdomains bounded inside the pores. Water in the narrowest pores melts at lower temperatures compared to that of volumetric water. This process can be mathematically described by the Gibbs–Thomson (GT) equation taking into account the dependence between the decrease of melting point of ice within the cylindrical pore of radius  $R_p$  [24, 29, 37, 38, 40, 41]:

$$R_p/\text{nm} = 0.68 - [k_{GT}/(T_m - T_{m0})] \quad (1)$$

where  $T_m$  and  $T_{m0}$  denote the melting point of the ice in the pores and outside them, respectively,  $k_{GT}$  is a constant (here  $k_{GT} = 32.33$  K  $\times$  nm). The curve of pore volume distribution (PSD)  $dV/dR$  can be determined from the DSC melting curves:

$$dV/dR/\text{cm}^3 \text{ nm}^{-1} \text{ g}^{-1} = [dq/dt(T_m - T_{m0})^2]/[k_{GT} \rho \beta m \Delta H(T)] \quad (2)$$

where  $dq/dt$ ,  $\rho$ ,  $\beta$ ,  $m$  and  $\Delta H(T)$  denote the DSC heat flow, the water density, the heating rate, the sample mass and the melting enthalpy of water, respectively. The  $\Delta H$  values as a function of temperature can be estimated as follows:

$$\Delta H(T)/\text{J g}^{-1} = 332 + 11.39(T_m - T_{m0}) + 0.155(T_m - T_{m0})^2 \quad (3)$$

TEM micrographs of carbosil samples were made using a BS 540 (Tesla) apparatus (accelerating voltage 80 kV, resolution 0.8 nm and magnification 24000 $\times$ ). Microscope samples were prepared using the platinum–carbon replication method with evaporation of platinum and a low amount of carbon onto the adsorbents, then treated with hydrofluoric acid to dissolve silica gel.

SEM micrographs were made using a scanning electron microscope Phenom (Fei, USA). The cathode CeB $_6$  as the electron source, and the BSE detector was used in the

**Fig. 1** Changes of structural parameters  $S_{\text{BET}}$  (a),  $V_p$  (b) and  $R_{\text{av}}$  (c) for the materials modified by various procedures

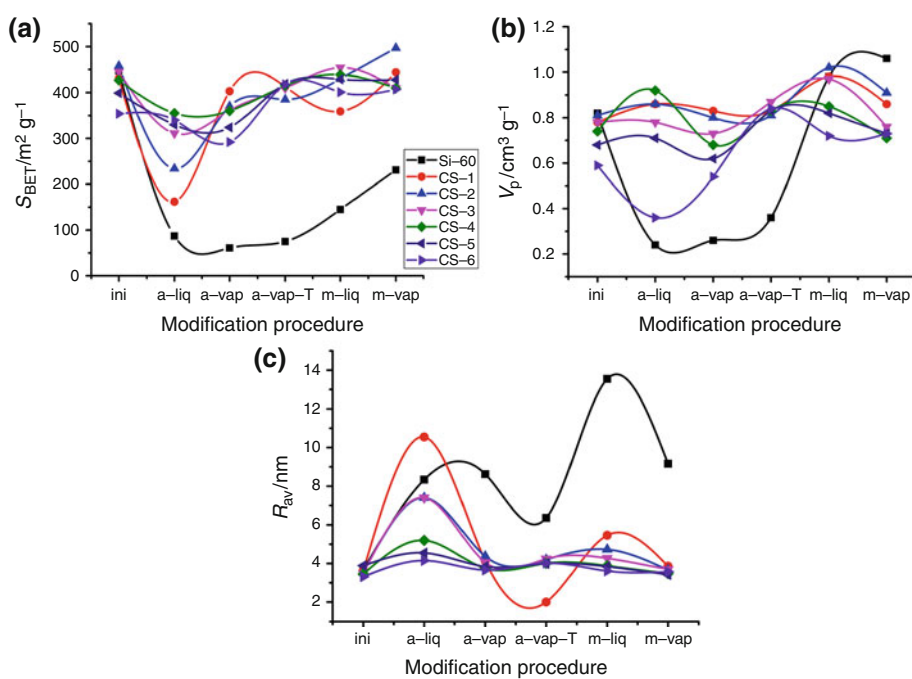


**Table 1** Structural parameters for the initial silica gel after hydrothermal treatment using various procedures and after thermal treatment

Adsorbent	$S_{\text{BET}}/\text{m}^2 \text{g}^{-1}$	$S_{\text{nano}}/\text{m}^2 \text{g}^{-1}$	$S_{\text{meso}}/\text{m}^2 \text{g}^{-1}$	$S_{\text{macro}}/\text{m}^2 \text{g}^{-1}$	$V_p/\text{cm}^3 \text{g}^{-1}$	$V_{\text{nano}}/\text{cm}^3 \text{g}^{-1}$	$V_{\text{meso}}/\text{cm}^3 \text{g}^{-1}$	$R_{\text{av}}/\text{nm}$
Si-60 <sub>ini</sub>	465	1.2	463.4	0	0.854	0.001	0.852	3.7
Si-60 <sub>a-liq</sub>	87	22.7	28.9	35.1	0.645	0.008	0.027	8.3
Si-60 <sub>a-vap</sub>	61	4.6	36.7	20	0.427	0.002	0.101	8.6
Si-60 <sub>m-liq</sub>	145	21.6	102.9	20.9	1.020	0.007	0.702	13.6
Si-60 <sub>m-vap</sub>	231	35.6	195.2	0.6	1.081	0.011	1.046	9.2
Si-60 <sub>a-vap-T</sub>	75	13.1	42.2	19.7	0.389	0.004	0.055	6.4
CS-1 <sub>a-vap-T</sub>	413	47	366.1	0.2	0.83	0.003	0.825	4.1
CS-2 <sub>a-vap-T</sub>	385	40.4	345.4	0.2	0.82	0.005	0.81	4.2
CS-3 <sub>a-vap-T</sub>	410	46.8	363.9	0.1	0.873	0.002	0.867	4.2
CS-4 <sub>a-vap-T</sub>	415	42.6	372.3	0.1	0.834	0.003	0.829	3.4
CS-5 <sub>a-vap-T</sub>	419	46.3	373.3	0.1	0.838	0.004	0.834	4.0
CS-6 <sub>a-vap-T</sub>	418	44.8	373.4	0.1	0.849	0.004	0.839	4.0

investigations. The samples were examined at a magnification of 5000 $\times$ .

## Results and discussion

Figure 1a–c presents the course of the changes of structural parameters  $S_{\text{BET}}$ ,  $V_p$  and  $R_{\text{av}}$  determined from the data of nitrogen adsorption/desorption isotherms for the initial materials and those hydrothermally modified under different conditions (water vapour/liquid water) using various sources of energy (classical autoclave or microwave reactor). As follows from the analysis of the scheme in Fig. 1, the structural parameters of silica gel change significantly

regardless of the modifier phase kind (liquid/vapour) and the kind of heat source (Fig. 1a–c; Table 1). For all modified silica gel samples, there is found a decrease in the specific surface area  $S_{\text{BET}}$  compared to that of initial silica (Fig. 1a), whereby these changes are more intensive for the samples modified in the classical autoclave.

There was made a detailed analysis of silica gel pores structure assuming their cylindrical shape. The external surface area of the initial silica gel is very small ( $S_{\text{macro}}$ , Table 1). The surface of particles is rather smooth, but after the HTT treatment the external surface slightly increases, however, it remains much smaller than the internal surface specific area ( $S_{\text{nano}}$ ,  $S_{\text{meso}}$ , Table 1). At the same time due to intensive silica transport during HTT,  $S_{\text{BET}}$  decreases

**Table 2** Structural parameters for the initial and hydrothermally modified carbosils

Adsorbent	$C_C/\%$	$S_{BET}/m^2 g^{-1}$	$S_{nano}/m^2 g^{-1}$	$S_{meso}/m^2 g^{-1}$	$S_{macro}/m^2 g^{-1}$	$V_p/cm^3 g^{-1}$	$V_{nano}/cm^3 g^{-1}$	$V_{meso}/cm^3 g^{-1}$	$R_{av}/nm$
CS-1 <sub>ini</sub>	1.8	431	59.3	371.4	0.1	0.784	0.002	0.799	3.46
CS-2 <sub>ini</sub>	2.5	458	90.4	367.5	0.1	0.81	0.052	0.754	3.54
CS-3 <sub>ini</sub>	6.0	445	91.3	353.9	0	0.78	0.052	0.726	3.50
CS-4 <sub>ini</sub>	8.3	427	92.7	334.1	0	0.738	0.051	0.686	3.46
CS-5 <sub>ini</sub>	13.1	399	91.5	307.3	0	0.675	0.050	0.625	3.89
CS-6 <sub>ini</sub>	18.9	354	61	293.2	0	0.615	0.022	0.591	3.31
CS-1 <sub>a-liq</sub>	1.8	162	44.9	116.8	0.6	0.875	0.024	0.815	10.55
CS-2 <sub>a-liq</sub>	2.6	234	56.7	170.3	6.7	0.877	0.021	0.586	7.4
CS-3 <sub>a-liq</sub>	6.3	311	52.8	257.7	0.1	0.790	0.014	0.770	7.4
CS-4 <sub>a-liq</sub>	8.4	355	57.3	298.0	0.2	0.925	0.015	0.904	5.2
CS-5 <sub>a-liq</sub>	13.3	330	66.1	263.5	0.3	0.768	0.019	0.737	4.6
CS-6 <sub>a-liq</sub>	20.0	340	71.6	268.8	0.2	0.721	0.018	0.689	4.17
CS-1 <sub>a-vap</sub>	1.9	403	60.6	324.0	0.1	0.832	0.006	0.821	4.13
CS-2 <sub>a-vap</sub>	2.8	370	51.4	318.3	0	0.809	0.027	0.782	4.37
CS-3 <sub>a-vap</sub>	6.3	361	58.9	302.2	0.1	0.737	0.009	0.723	4.06
CS-4 <sub>a-vap</sub>	8.8	360	60.5	299.6	0.1	0.677	0.019	0.652	3.75
CS-5 <sub>a-vap</sub>	13.3	324	60	264.5	0	0.623	0.020	0.602	3.84
CS-6 <sub>a-vap</sub>	19.4	292	59.7	232.6	0	0.536	0.012	0.522	3.66
CS-1 <sub>m-liq</sub>	1.8	359	43.2	315.7	0.3	0.983	0.007	0.965	5.46
CS-2 <sub>m-liq</sub>	3.0	430	48.3	381.9	0.1	1.019	0.013	1.004	4.73
CS-3 <sub>m-liq</sub>	6.6	454	54.3	399.3	0.2	0.981	0.010	0.959	4.27
CS-4 <sub>m-liq</sub>	9.2	439	55.1	384.3	0.1	0.851	0.004	0.846	3.88
CS-5 <sub>m-liq</sub>	13.9	429	60.3	368.3	0.1	0.826	0.008	0.814	3.84
CS-6 <sub>m-liq</sub>	21.5	401	64.4	336.0	0.4	0.747	0.012	0.719	3.61
CS-1 <sub>m-vap</sub>	2.0	444	52	392.1	0.1	0.859	0.004	0.852	3.86
CS-2 <sub>m-vap</sub>	3.3	497	48.7	447.7	0.2	0.91	0.001	0.905	3.68
CS-3 <sub>m-vap</sub>	6.5	410	46.4	363.3	0.1	0.755	0.004	0.769	3.69
CS-4 <sub>m-vap</sub>	8.9	410	44.4	365.8	0.2	0.714	0	0.709	3.48
CS-5 <sub>m-vap</sub>	13.6	428	49.8	377.6	0.1	0.732	0.002	0.727	3.42
CS-6 <sub>m-vap</sub>	19.3	407	40.7	366.6	0.2	0.729	0.001	0.724	3.57

remarkably. Such modification in the presence of water molecules (particularly liquid water) creates a small quantity of nano-sized pores ( $V_{nano}$ , Table 1). The analysis of contribution of different types of pores to the total porosity indicates that cylindrical pores are predominant in all studied systems.

The pore volume of silica gels ( $V_p$ , Fig. 1b;  $V_{meso}$ , Table 1) decreases after modification in the autoclave, but increases after treatment in the microwave reactor. Generally, HTT causes the increase in pore sizes ( $R_{av}$ , Fig. 1c; Table 1), and the most intensive changes are observed for all samples modified in the microwave reactor under the water layer.

In the case of thermally modified carbosils (series CS- $x_{a-vap-T}$ ), no significant changes in the porous structure were observed (Table 1). This points to the fact that the layer of carbon deposited on the initial surface extensively

restrains modifying agent (water vapour) access to the silica surface. The obtained materials have a small number of pores of the size  $R < 1$  nm ( $S_{nano}$ ,  $V_{nano}$ , Table 1), but the remaining contribution is made by a largely developed structure of mesopores ( $S_{meso}$ ,  $V_{meso}$ , Table 1).

Similar changes, but of significantly smaller intensity are observed for the initial and modified carbosils. All carbosils are mesoporous materials with a small contribution of nanopores ( $S_{nano}$ ,  $V_{nano}$ ,  $S_{meso}$ ,  $V_{meso}$ , Table 2). The analysis of the curves in Fig. 1a indicates drop of the specific surface area  $S_{BET}$  for the carbosils modified in the autoclave and smaller rise for the samples modified in the microwave reactor. This shows that the carbon deposit on the surface of carbosils significantly affects intensity and character of structural parameter changes. The extent of  $S_{BET}$  changes in the analysed series of adsorbents is inversely proportional to the carbon deposit content

**Fig. 2** Curves of pores volume distribution obtained from the nitrogen desorption isotherm data for the series of silica gels (a) and carbosils of the series CS-1 (b) and CS-6 (c) initial and hydrothermally modified using various procedures

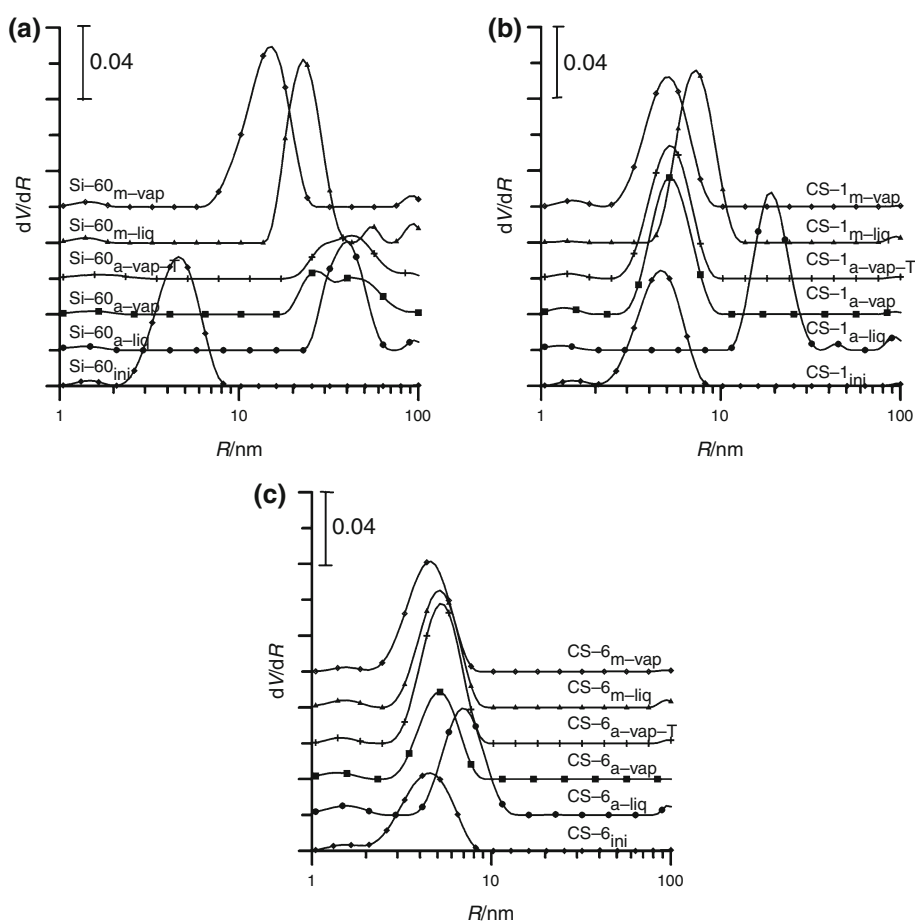


(Fig. 1a; Table 2). This means that the carbon deposit restrains the modifying agent access to the silica matrix surface of the studied materials. The dependences concerning the changes of pore volume for carbosils ( $V_p$ , Fig. 1b; Table 2) indicate that modification in the microwave reactor seems to be more effective, but treatment in the classical autoclave is more advantageous for increase of their sizes ( $R_{av}$ , Fig. 1c; Table 2). For the carbosils of smaller carbon deposit content (1.8–6 %  $C_C$ , the series CS-1 to CS-3), changes of  $S_{BET}$ ,  $V_p$  and  $V_{av}$  are quite large. However, with the increase in the deposit amount (8.3–19 %  $C_C$ , the series CS-4 to CS-6), changes of the parameters under consideration are smaller. This is a result of more intensive suppression of silica surface against the action of water molecules during the HTT (Fig. 1a–c; Table 2).

In the case of all series of carbosils it was found that each procedure causes different changes within pores structure. In most cases the contribution of nanopores surface increases with the increasing carbon deposit content ( $S_{nano}$ ,  $V_{nano}$ , Table 2). This suggests hydrothermal modification of carbonaceous part of carbosils.

Figure 2a presents the curves of pore volume distribution in relation to the radii ( $dV/dR = f(R)$ ) for silica gels

(Fig. 2a), and the exemplary carbosils of minimal and maximal carbon deposit contents (series CS-1, Fig. 2b and CS-6, Fig. 2c) of the initial and hydrothermally modified ones. As follows from the analysis of the curves, all modified adsorbents are mesoporous materials with small contribution of nanopores. Hydrothermal modification of gels caused significant changes of porous structure (Fig. 2a) which clearly shows the impact of different procedures and conditions of HTT on porosity of the obtained materials. Modification in the microwave reactor causes two and in the autoclave even three times increase of pore sizes compared to the initial silica gel. The maxima on the PSD curve for silica gels are present in a wide range of  $R_{av}$ . However, the position of peaks on the curves of pore distribution for carbosils confirms the screening effect of carbon deposit on possibility of porous structure changes during the HTT process. The maxima on the PSD curves of CS-1 series (Fig. 2b) are more differentiated and shifted towards larger size pores than it is observed for the carbosils of CS-6 series. In this case (Fig. 2c) the maxima of PSD curves have similar values. This means that the deposit significantly restricts access of a modifying agent to the mineral matrix. The results of curves analysis are consistent with the structural parameters presented in Tables 1 and 2.

**Fig. 3** DSC curves of ice melting for the initial adsorbents (a) and silica gels obtained after the thermal treatment (series CS- $x_{a-vap-T}$ ) (b)

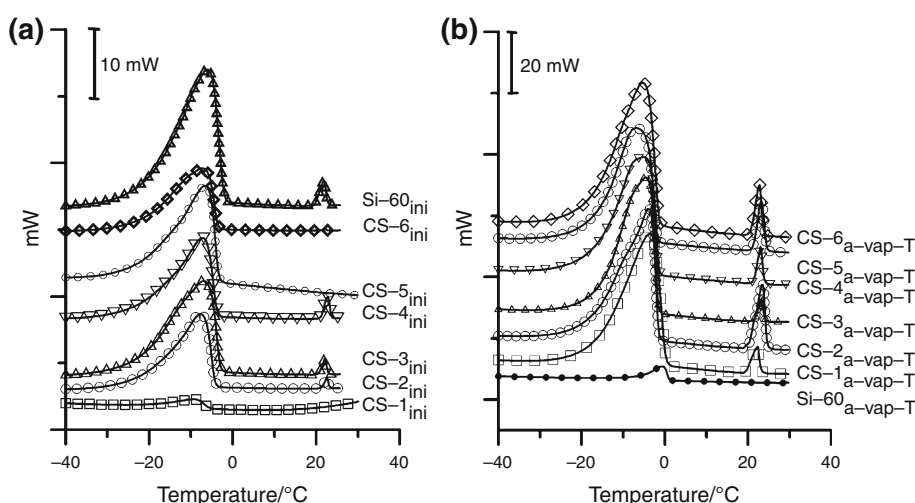


Figure 3 presents the exemplary DSC curves of ice melting in the initial carboxils (series CS- $x_{ini}$ , Fig. 3a) and thermally modified (series CS- $x_{a-vap-T}$ , Fig. 3b) samples. The curves of the similar course were also registered for the other series of adsorbents. As follows from the comparison of the DSC curves for the silica gel (Si-60 $_{ini}$ ) and initial carboxils samples (Fig. 3a), carbon deposition in the silica pores causes slight shift of temperatures of ice melting peaks towards lower temperatures compared to the peak registered for the initial silica (Si-60 $_{ini}$ ). This effect is connected with the decrease in pore size as a result of carbonization. This is consistent with the size of structural parameters obtained from the low-temperature nitrogen adsorption/desorption isotherms data (Tables 1, 2). As follows from the data in the tables, hydrothermal modification in saturated water vapours causes significant changes in the porous structure of the initial silica, but the effects are smaller for the carboxil samples. A significant dependence is found for the samples modified under the liquid water layer. In this case there was found distinct conformity in the shift of  $T_{onset}$  and  $T_{max}$  towards lower temperature with the increasing carbon deposit content for the hydrothermally modified samples using microwaves.

The effect of characteristic temperatures  $T_{onset}$  shift towards lower temperatures in relation to the signal registered for silica gel is distinct for the peaks of ice melting in the carbon deposit free samples due to thermal modifications (series CS- $x_{a-vap-T}$ , Fig. 3b; Tables 1, 2). Figure 3b shows distinctly the tendency to shift the characteristic temperatures  $T_{onset}$  towards the temperature registered for the modified silica gel (Si-60 $_{a-vap-T}$ ) depending on the content of carbon deposit  $C_C$  in the modified carboxils. The tendency to decrease melting temperature ( $T_{onset}$  and  $T_{max}$ ) of the ice in the pores of the studied silica gels and carboxils is well seen in Fig. 4. It should be noted that changes of  $T_{onset}$  (Fig. 4a) refer to the process of melting ice in

pores with a size of  $R_{min}$ . These changes correlate well with an increase in the participation of nanopores with increasing of the carbon deposit in the studied materials (Tables 1, 2). While the average pore size  $R_{av}$  in the series of adsorbents does not change so significantly (Tables 1, 2), which was also confirmed in the course of the curves in Fig. 4b.

Figure 5 presents the curves of pore volume distribution towards their effective radii ( $dV/dR = f(R_{av})$ ) obtained from the DSC curves for the initial or hydrothermally modified silica gels (Fig. 5a) and carboxils from the series CS-1 (Fig. 5b) and CS-6 (Fig. 5c). The analysis of the presented curves indicates that application of each procedure leads to essential changes in the porous structure of the studied materials. These changes are the most intensive for the silica gel series (Fig. 5a), and their intensity decreases for the carboxils with the increasing amount of carbon deposit. The least intensive effect of hydrothermal modification is observed for the carboxils of the maximal carbon deposit content (Fig. 5c). These observations are consistent with the structural parameters of the materials under consideration for both initial materials and those modified by various research procedures. Moreover, there was found large conformity of peaks positions on the presented PSD curves (Fig. 5) with those on the  $dV/dR = f(R_{av})$  curves obtained from the nitrogen desorption data (Fig. 2). The observed differences in the course of these curves are due to the limited access of the media ( $N_2$ ,  $H_2O$ ) into the pores of the tested materials. These limitations are due to different sizes of the particles and different nature of interactions with the surface.

The TEM micrographs of some initial carboxils (Fig. 6) show the difference in the distribution of the carbon deposit on the surface of the silica matrix, depending on its quantity. The surface of the samples with a small amount of carbon deposit (CS-2 $_{ini}$ , Fig. 6a) is smooth and uniform

**Fig. 4** Changes of  $T_{\text{onset}}$  (a) and  $T_{\text{max}}$  (b) for silica gels and carbosils of the increasing carbon deposit contents modified under different conditions of the HTT process

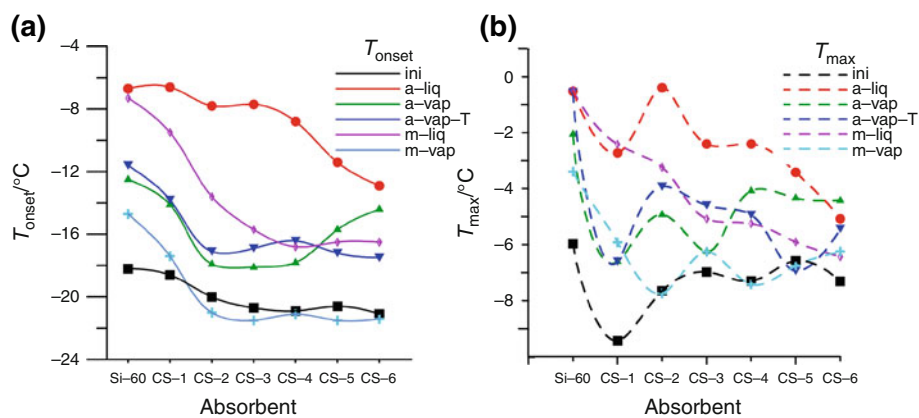
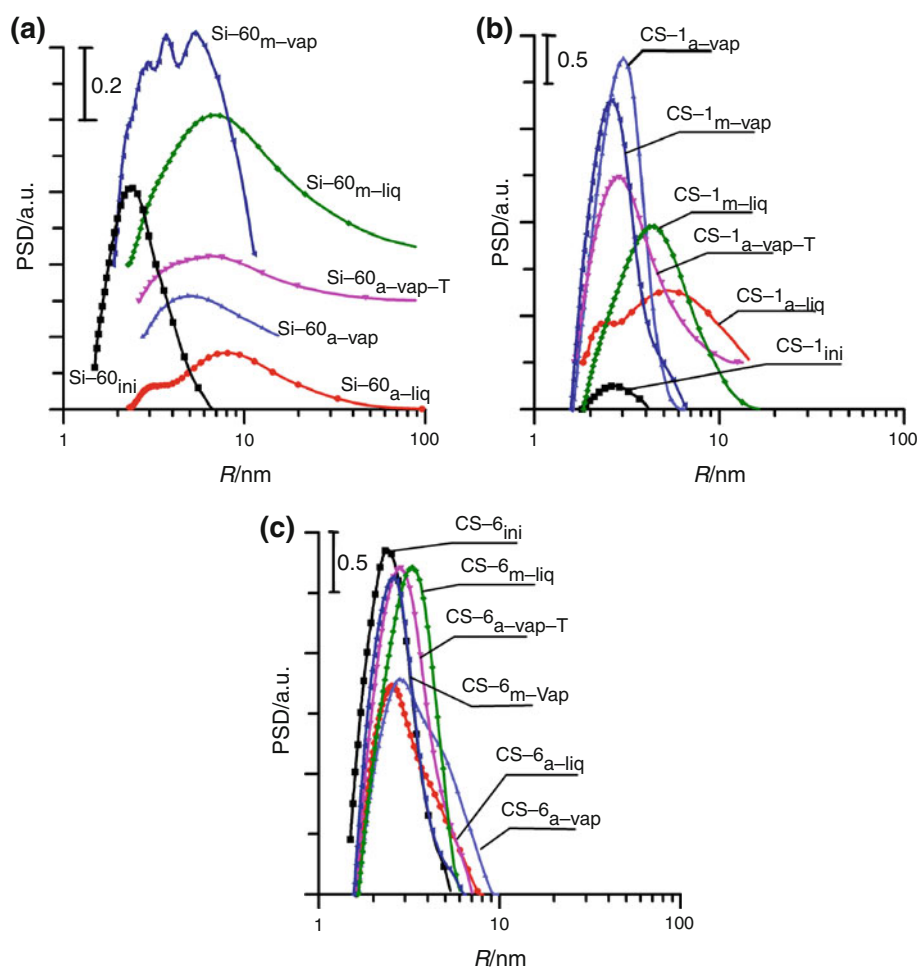


**Fig. 5** Pore size distribution (PSD) curves obtained from the DSC curves for the series of silica gels (a) and carbosils of the series CS-1 (b) and CS-6 (c) hydrothermally modified using various procedures



and the deposit is evenly distributed. With the increase of  $C_c$  (CS-5<sub>ini</sub>, Fig. 6b), additional clustering of pyrocarbon can be seen, but some areas of silica uncovered by carbon deposit are still visible. The largest clusters of pyrocarbon are observed on the surface of the sample containing a maximum carbon deposit content (CS-6<sub>ini</sub>, Fig. 6c). Moreover, the SEM analysis of the samples thermally modified (series CS- $x$ <sub>a-vap-T</sub>, Fig. 7) shows clearly

differences in the surface structure of thermally modified samples. They result from the blocking of the silica matrix by carbon deposit. Blocking was most effective in the case of the samples with the highest content of carbon deposit (CS-6<sub>a-vap-T</sub>, Fig. 7c). Significant unevenness and roughness of the surface of the sample containing a minimum content of the deposit (CS-1<sub>a-vap-T</sub>, Fig. 7a) are gradually smoothed (CS-4<sub>a-vap-T</sub>, Fig. 7b) to obtain a mineral matrix



**Fig. 6** TEM micrographs of CS-2<sub>ini</sub> (a), CS-5<sub>ini</sub> (b) and CS-6<sub>ini</sub> (c)

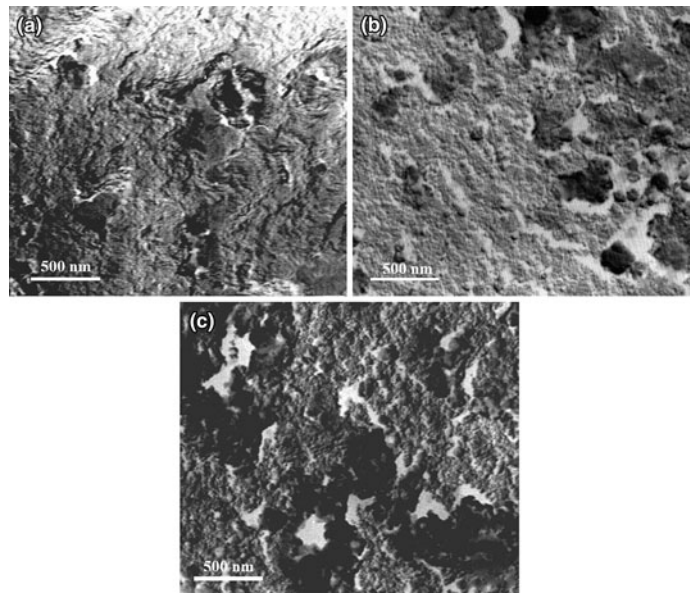
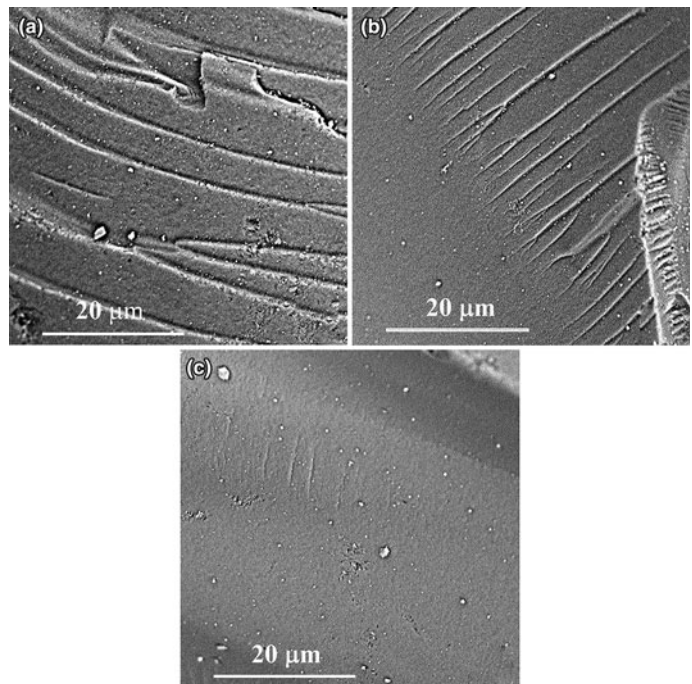


**Fig. 7** SEM micrographs of CS-1<sub>a-vap-T</sub> (a), CS-4<sub>a-vap-T</sub> (b) and CS-6<sub>a-vap-T</sub> (c)



of smoothed surface (CS-6<sub>a-vap-T</sub>, Fig. 7c). This indicates that the carbon deposit blocks the access of modifying agent (H<sub>2</sub>O) to the mineral matrix and correlates closely with the carbon deposit content.

## Conclusions

As follows from the studies, hydrothermal modification of silica gel and carbosils of different carbon deposit contents

causes essential changes in porous structure of the studied materials. Hydrothermal modification of the initial silica gel Si-60<sub>ini</sub> under the described conditions caused significant lowering in the specific surface area  $S_{BET}$  and rise in the average pore radius ( $R_{av}$ ). Changes of the modified silica gel pore volumes  $V_p$  depend on the modification way.

Carbon deposition on the silica gel surface causes at first increase (with low contents of carbon deposit) and then decrease of the specific surface area and porosity (both volume and size of pores) of the studied carbosils. Intensity

of these changes depends on the carbon deposit content. Decrease of pore size is confirmed by the shift of the melting peaks of ice inside the carbosil pores towards lower temperatures compared to the parameters obtained for the initial silica gel.

The microscopic investigations show that the carbon deposit layer on the silica surface covers the silica matrix efficiently. The changes of structural parameters of carbon-silica adsorbents are less intense than those observed for the initial silica gel. In the case of carbosils of small carbon deposit contents, the parameters  $S_{\text{BET}}$  and  $R_p$  change significantly due to the presence of a thin layer of carbon deposit distributed in the silica mesopores. For the carbosils of larger deposit contents, these changes are smaller, which is a result of larger surface suppression against the action of water molecules during the HTT.

The presented results of the studies are compatible with the structural parameters obtained using various analytical methods and confirmed applicability of the DSC method to study porous structure of the modified silica gels and carbosils.

**Open Access** This article is distributed under the terms of the Creative Commons Attribution License which permits any use, distribution, and reproduction in any medium, provided the original author(s) and the source are credited.

## References

1. Gun'ko VM, Lebeda R. Carbon-silica adsorbents. In: Hubbar AT, editor. Encyclopedia of surface and colloid science. New York: Marcel Dekker; 2002. p. 864–78.
2. Kamegawa K, Yoshida H. A method for measuring surface area of carbon of carbon-coated silica gel. *Bull Chem Soc Jpn.* 1009;63:3683–5.
3. Skubiszewska-Zięba J, Lebeda R, Gun'ko VM, Charmas B. Structural and adsorption characteristics of pyrocarbon-mineral adsorbents. In: Blitz JP, Gun'ko VM, editors. Surface chemistry in biomedical and environmental science. NATO science series II: mathematics, physics and chemistry. Berlin: Springer; 2006. p. 123–34.
4. Mel'gunov M, Fenelonov VB, Lebeda R, Charmas B. Applicability of verification for a new method of measuring the components of surface areas in bicomponent catalysts and adsorbents. *J Colloid Interface Sci.* 2001;39:357–67.
5. Skubiszewska-Zięba J, Charmas B, Lebeda R, Tertykh VA, Yanishpolskii VV. Complex investigations of structural and thermal properties of silica-titania adsorbents. *J Therm Anal Calorim.* 2012;108:1085–92.
6. Charmas B, Lebeda R, Gérard G, Villiéras F. Effect of oxidation on surface heterogeneity of carbosils. *Appl Surf Sci.* 2002;196:126–37.
7. Lebeda R, Turov VV, Charmas B, Skubiszewska-Zięba J, Gun'ko VM. Surface properties of mesoporous carbon-silica adsorbents. *J Colloid Interface Sci.* 2000;223:112–25.
8. Lebeda R. Carbon-mineral adsorbents—new type of sorbents? part I. The methods of preparation. *Mater Chem Phys.* 1992;31:243–55.
9. Lebeda R. Carbon-mineral adsorbents—new type of sorbents part II. Surface properties and methods of their modification. *Mater Chem Phys.* 1993;34:123–41.
10. Lebeda R, Dąbrowski A. Adsorption on new modified inorganic sorbents. Amsterdam: Elsevier; 1996. p. 15.
11. Lebeda R, Mendyk E, Tertykh VA. Effect of the hydrothermal treatment method in an autoclave on the silica gel porous structure. *Mater Chem Phys.* 1995;42:7–11.
12. Lebeda R, Tertykh VA, Sidorchuk VV, Skubiszewska-Zięba J. Peculiarities of steam-phase hydrothermal modification of pyrogenic silicium dioxide. *Colloid Surf A.* 1998;135:253–65.
13. Lebeda R, Mendyk E, Gierak A, Tertykh VA. Hydrothermal modification of silica gels (xerogels). 1. Effect of treatment temperature on their porous structure. *Colloid Surf A.* 1995;105:181–9.
14. Lebeda R, Mendyk E, Gierak A, Tertykh VA. Hydrothermal modification of silica gels (xerogels). 2. Effect of the duration of treatment on their porous structure. *Colloid Surf A.* 1995;105:191–7.
15. Lebeda R, Mendyk E, Tertykh VA. Effect pH of medium on hydrothermal treatment of silica gel (xerogels) in an autoclave. *Mater Chem Phys.* 1995;43:53–8.
16. Skubiszewska-Zięba J. The impact of microwave energy on the results of silica gel hydrothermal modification. *Adsorption.* 2010;16:485–93.
17. Charmas. TG and DSC studies of bone tissue. Effects of osteoporosis. *Thermochim Acta.* 2013. doi:10.1016/j.tca.2013.08.032.
18. Majda D, Makowski W, Manko M. Pore size distribution of micelle-templated silicas studied by thermoporosimetry using water and *n*-heptane. *J Therm Anal Calorim.* 2012;109:663–9.
19. Hatakeyama T, Inui Y, Iijima M, Hatakeyama H. Bound water restrained by nanocellulose fibres. *J Therm Anal Calorim.* 2013;113:1019–25.
20. Yan X, Wang TB, Pei HR, Wang LP, Lan XZ. Phase behavior of dodecane-tridecane mixtures confined in SBA-15. *J Therm Anal Calorim.* 2013;113:1297–302.
21. Skubiszewska-Zięba J. Structural and energetic properties of carbosils hydrothermally treated in the classical autoclave or the microwave reactor. *Adsorption.* 2008;14:695–709.
22. Ishikiriya K, Todoki M. Pore size distribution measurements of silica gels by means of differential scanning calorimetry. I. Optimization for determination of PSD. *J Colloid Interface Sci.* 1995;170:92–102.
23. Ishikiriya K, Todoki M. Pore size distribution measurements of silica gels by means of differential scanning calorimetry. II. Thermoporosimetry. *J Colloid Interface Sci.* 1995;171:103–11.
24. Książczak A, Radomski A, Zielenkiewicz T. Nitrocellulose porosity—thermoporometry. *J Therm Anal Calorim.* 2003;74:559–68.
25. Landry MR. Thermoporometry by differential scanning calorimetry: experimental considerations and applications. *Thermochim Acta.* 2005;433:27–50.
26. Yamamoto T, Endo A, Inagi Y, Ohmori T, Nakaiwa M. Evaluation of thermoporometry for characterization of mesoporous materials. *J Colloid Interface Sci.* 2005;284:614–20.
27. Endo A, Yamamoto T, Inagi Y, Iwakabe K, Ohmori T. Characterization of nonfreezable pore water in mesoporous silica by thermoporometry. *J Phys Chem C.* 2008;112:9034–9.
28. Riikonen J, Salonen J, Lehto VP. Utilising thermoporometry to obtain new insights into nanostructured materials. *J Therm Anal Calorim.* 2011;105:811–30.
29. Brun M, Lallemand A, Quinson J, Eyraud C. A new method for simultaneous determination of size and shape of pores: the thermoporometry. *Thermochim Acta.* 1977;21:59–88.
30. Gun'ko VM, Turov VV. Nuclear magnetic resonance studies of interfacial phenomena. New York: Taylor & Francis; 2013.
31. Gun'ko VM, Turov VV, Bogatyrev VM, Zarko VI, Lebeda R, Goncharuk EV, Novza AA, Turov AV, Chuiko AA. Unusual properties of water at hydrophilic/hydrophobic interfaces. *Adv Colloid Interface Sci.* 2005;118:125–72.
32. Gregg SJ, Sing KSW. Adsorption, surface area and porosity. London: Academic Press; 1991. p. 303.

33. Gun'ko VM. Consideration of the multicomponent nature of adsorbents during analysis of their structural and energy parameters. *Theor Exp Chem*. 2000;36:319–24.
34. Nguyen C, Do DD. Effect of probing vapors and temperature on the characterization of micro-mesopore size distribution of carbonaceous materials. *Langmuir*. 2000;16:7218–22.
35. Gun'ko VM, Leboda R, Skubiszewska-Zięba J, Zarko VI, Goncharuk EV, Charmas B, Mikhalovskiy SV. Comparative analysis of porous structure and adsorption properties of activated carbons. *Chem Phys Technol Surf*. 2012;2:123–32.
36. Gun'ko VM, Turov VV, Leboda R, Skubiszewska-Zięba J, Charmas B. Confined space effects driving to heterogenization of solutions at the interfaces. *Adsorption*. 2013;19:305–21.
37. Gun'ko VM, Mikhalovsky SV. Evaluation of slitlike porosity of carbon adsorbents. *Carbon*. 2004;42:843–9.
38. Gun'ko VM, Leboda R, Skubiszewska-Zięba J. Heating effects on morphological and textural characteristics of individual and composite nanooxides. *Adsorption*. 2009;15:89–98.
39. Savina IN, Gun'ko VM, Turov VV, Dainiak M, Phillips GJ, Galaev IYu, Mikhalovsky SV. Porous structure and water state in cross-linked polymer and protein cryo-hydrogels. *Soft Matter*. 2011;7:4276–83.
40. Gun'ko VM, Savina IN, Mikhalovsky SV. Cryogels: morphological, structural and adsorption characterisation. *Adv Colloid Interface Sci*. 2013;187-188:1–46.
41. Kjeldsen AM, Geiker MR. On the interpretation of low temperature calorimetry data. *Mater Struct*. 2008;41:213–24.